Hyperactivation of Nrf2 leads to hypoplasia of bone *in vivo*

Eiki Yoshida[1,4], Takafumi Suzuki[1,4]*, Masanobu Morita[1,4], Keiko Taguchi[1], Kohei Tsuchida[1], Hozumi Motohashi[2], Minoru Doita[3], and Masayuki Yamamoto[1]*

[1]Department of Medical Biochemistry, Tohoku University Graduate School of Medicine, 2-1 Seiryo-machi, Aoba-ku, Sendai 980-8575, Japan.
[2]Department of Gene Expression Regulation, Institute of Development, Aging, and Cancer, Tohoku University, 4-1 Seiryo-machi, Aoba-ku, Sendai 980-8575, Japan.
[3]Department or Orthopaedic Surgery, Iwate Medical University, 19-1 Uchimaru, Morioka, Iwate 020-8505, Japan.
[4]These authors contributed equally to this work.

*Corresponding author: Masayuki Yamamoto or Takafumi Suzuki
Department of Medical Biochemistry,
Tohoku University Graduate School of Medicine,
2-1, Seiryo-machi, Aoba-ku, Sendai, 980-8575, Japan
TEL 81-22-717-8084,
FAX 81-22-717-8090
E-mail: masiyamamoto@med.tohoku.ac.jp or taka23@med.tohoku.ac.jp

Running title; Nrf2 suppresses bone formation

Keywords: Nrf2, Keap1, bone, osteoblast,

Abstract

Keap1 is a negative regulator of Nrf2, a master transcription factor that regulates cytoprotection against oxidative and electrophilic stresses. Although several studies have suggested that the Keap1-Nrf2 system contributes to bone formation besides the maintenance of redox homeostasis, how Nrf2 hyperactivation by Keap1-deficiency affects the bone formation remains to be explored, as the *Keap1*-null mice are juvenile lethal. To overcome this problem, we utilized viable Keap1-deficient mice that we have generated by deleting the esophageal Nrf2 in *Keap1*-null mice (NEKO mice). We found that the NEKO mice exhibit small body size and low bone density. Although nephrogenic diabetes insipidus has been observed in both the NEKO mice and renal specific Keap1-deficient mice, the skeletal phenotypes are not recapitulated in the renal specific Keap1-deficient mice, suggesting that the skeletal phenotype by Nrf2 hyperactivation is not related to the renal phenotype. Experiments with primary culture cells derived from *Keap1*-null mice showed that differentiation of both osteoclasts and osteoblasts were attenuated, demonstrating that impaired differentiation of osteoblasts rather than osteoclasts is responsible for bone hypoplasia caused by Nrf2 hyperactivation. Thus, we propose that the appropriate control of Nrf2 activity by Keap1 is essential for maintaining bone homeostasis.

(194/200 words)

Introduction

Bone homeostasis is believed to be maintained on the balance between formation and resorption mediated by osteoblasts and osteoclasts, respectively (Manolagas, 2000). Reactive oxygen species (ROS) have been implicated as an important factor regulating the bone homeostasis. Several *in vitro* and *in vivo* studies reported that increased oxidative stress shows negative effects on bone formation by modulating differentiation and survival of osteoblasts (Mody et al, 2001; Lean et al, 2003; Bai et al, 2004; Jun et al, 2008). Clinical studies have also demonstrated that dysregulation of the antioxidant system and subsequent ROS accumulation are both important mediators of bone loss (Asagiri and Takayanagi, 2007). However, it remains to be clarified how oxidative stresses induce bone loss.

Transcription factor Nrf2 (nuclear factor erythroid 2-related factor 2) plays a key role in the cytoprotection from oxidative stress and xenobiotic stress (Itoh et al, 1997; Suzuki et al, 2013). Under unstressed conditions, Nrf2 protein level is maintained at low level as Nrf2 is ubiquitinated by Keap1 (Kelch-like ECH-associated protein 1)-based ubiquitin E3 ligase complex and degraded by the proteasome (Itoh et al, 1999; Kobayashi et al, 2004; Suzuki and Yamamoto, 2015). Upon the exposure to oxidative and/or xenobiotic stresses that inactivates Keap1, Nrf2 is stabilized and activates transcription of various cytoprotective genes, conferring resistance against the stresses (Suzuki and Yamamoto, 2017).

It has been reported that osteoclast differentiation is enhanced by Nrf2 deficiency (Hyeon et al, 2013) and suppressed by Nrf2 activation through deletion of Keap1 (Sakai et al, 2017), suggesting that Nrf2 suppress bone resorption and subsequently promote bone formation. In contrast, overexpression of Nrf2 negatively regulate osteoblastgenesis of MC3T3-E1 cells (Hinoi et al, 2006). Although these observations suggest that differentiation of both osteoclasts and osteoblasts is suppressed by Nrf2 activation, physiological effects of the Nrf2 activation on bone development have not been fully clarified yet.

Nrf2 is constitutively activated in Keap1-null mouse (Wakabayashi et al, 2003), so that the Keap1-null mouse is a good model for the understanding of physiological contribution of Nrf2 activation to bone homeostasis. However, juvenile lethal due to hyperkeratosis in the upper digestive tract, which leads to the obstruction of the

esophagus and death by starvation made it infeasible to assess the effects of Keap1-deficiency on bone homeostasis (Wakabayashi et al, 2003). In this study, therefore, we decided to utilize a viable mouse model harboring systemic activation of Nrf2, in which a squamous epithelium-specific Nrf2-deficiency in the context of systemic Keap1-deficiency (*Keap1*$^{-/-}$*::Nrf2*$^{Flox/Flox}$*::K5*-Cre or NEKO mice) corrects the hyperkeratosis of the esophagus, and subsequent lethality, while hyperactivation of Nrf2 is observed in most tissues, with the exception of the esophagus and skin (Suzuki *et al*, 2017). We found that NEKO mice exhibited small body size and low bone density. Experiments with primary cells derived from Keap1-null mice indicates that differentiation of both osteoclasts and osteoblasts is attenuated, indicating that Nrf2 activation inhibits differentiation of both osteoclasts and osteoblasts. These results support the notion that reduction of bone formation in NEKO mice is due to inhibition of osteoblast differentiation by Nrf2 activation and that Nrf2 activation lead to hypoplasia of bone mass by impairing differentiation of osteoblasts.

Results

NEKO mice exhibit bone hypoplasia

To investigate function of Nrf2 on bone development, we examined Keap1-null mice in which Nrf2 is constitutively activated. Because of their juvenile lethality due to hyperkeratosis of esophagus (Wakabayashi et al, 2003), it has been difficult to examine adult Keap1-null mice. We generated NEKO mice that are able to survive until adulthood. NEKO mice harbor hyperactivation of Nrf2 in most tissues with the exception of the esophagus and skin (Suzuki et al, 2017).

We first examined whole appearance of the mouse using X-ray photography (Fig 1A,B). The picture showed that NEKO mouse was smaller than control mouse, but skeletal malformation was not observed in NEKO mice (Fig 1A,B). This phenotype was not observed in the *Keap1*$^{-/-}$*::Nrf2*$^{-/-}$ mice (Wakabayashi et al, 2003), indicating that the skeletal phenotype is due to hyperactivation of Nrf2. Consistent with the small body of NEKO mice, femur length of NEKO mice is significantly smaller than that of control mice (Fig 1C,D), indicating the impaired growth of NEKO mice.

To further investigate bone mass, we examined femur of NEKO and control mice at age of 8-10 weeks by 3-dimensional reconstruction CT imaging (Fig. 2A,B). Whole appearance of femur from NEKO mice shows increased radiolucency and smaller bone size (Fig. 2A,B). Cross-section image of femur visually shows that thinner cortical bone and sparser trabecular bone in NEKO mice (Fig. 2C,D). Bone morphometric parameters were also assessed from proximal to distal area of femur with a μCT analysis program. Consistent with the 3-dimensional reconstruction imaging results, a dramatic decrease in cortical bone thickness (Ct. Th., Fig. 2E), volume bone mineral density (vBMD., Fig. 2F) and cortical bone tissue mineral density (CB. TMD., Fig. 2G) in NEKO mice.

The decrease of bone mass was reproducibly observed even in elder NEKO mice (Fig S1A-C). Showing very good agreement with the result of femur, three-dimensional reconstruction image of cranial bone displays that the radiolucency is increased in NEKO mice compared to control mice (Fig S2A-D), while no malformation in NEKO mice is observed (Fig S2A-D). Thickness of femur growth plate was not affected in NEKO mice although intensity of Alcian blue positive cartilage in growth plate tends to be decreased in NEKO mice (Fig S3), suggesting that chondrogenesis is also mildly

affected by Keap1 deficiency. In addition, blood ionized calcium level of NEKO mice was lower than that of control mice (Fig. 2H), indicating that the severe bone hypoplasia leads to reduction of blood ionized calcium level in NEKO mice. These results demonstrate that hyperactivation of Nrf2 leads to severe bone hypoplasia in mouse.

Bone hypoplasia of NEKO mice is not linked to their renal failure

Because NEKO mice display nephrogenic diabetes insipidus (Suzuki et al, 2017), we tested whether bone hypoplasia of NEKO mice is due to their renal dysfunction. To this end, we examined kidney-specific Keap1-deficient mice (*Keap1*$^{Flox/Flox}$*::Pax8*-rtTA::*tetO*-Cre, or Keap1 TKO mice), and treated the mice with DOX from the embryonic stage, by administration of DOX to the pregnant mother. The *Keap1* gene was specifically deleted in the renal tubular cells, and the Keap1 TKO mice displays nephrogenic diabetes insipidus, like NEKO mice (Suzuki et al, 2017). Femur length of Keap1 TKO mice is comparable to that of control mice (Fig. S3A,B). X-ray photography and 3-dimensional reconstruction imaging shows no different appearance between Keap1 TKO and control mice (Fig. S3C,D and S4A-D). In addition, there is no difference of bone morphometric parameters and blood ionized calcium level between Keap1 TKO and control mice (Fig. S4E-H), demonstrating that the severe bone hypoplasia in NEKO mice is not attributable to their renal dysfunction.

Nrf2 hyperactivation leads to perturbation of bone homeostasis

We next investigated how Keap1-deficiency affects the differentiation of osteoblasts and osteoclasts. First, we conducted *in vitro* differentiation experiments of osteoclasts using bone marrow (BM)-derived cells from NEKO and control mice. The BM cells were cultured in the medium supplemented with M-CSF and RANKL (Fig. 3A). After two-day pre-culture with M-CSF, RANKL was added to induce osteoclast differentiation. Five days after the induction, mature differentiated osteoclasts were visualized by TRAP staining. Whereas control BM cells produced the largest number of TRAP-positive multi-nucleated mature osteoclasts (Fig. 3B), NEKO mouse-derived BM cells produced fewer or practically no osteoclasts (Fig. 3C). This showed very good agreement with the previous report that osteoclast differentiation of splenic cells from

Keap1-deficient mice was impaired (Sakai et al, 2017). These results indicate that Nrf2 activation suppresses osteoclast differentiation.

Because NEKO mice showed severe bone hypoplasia despite the diminished osteoclast production from BM cells, we surmised that osteoblast differentiation might also be impaired in NEKO mice. To address this hypothesis, we conducted *in vitro* osteoblast differentiation experiment using newborn calvarias of *Keap1*$^{+/-}$ and *Keap1*$^{-/-}$ mice. Collected cells were pre-cultured for two days and induced to differentiate to osteoblasts by adding ascorbic acid, dexamethasone and β-glycerophosphate (Fig. 3D). Osteoblast differentiation was examined by measuring alkaline phosphatase (AP) staining. While the osteoblast differentiation of cells from *Keap1*$^{+/-}$ mice was nicely observed, that of *Keap1*$^{-/-}$ mice were severely impaired (Fig. 3E). Taken together, these results thus indicate that Nrf2 suppresses osteoblast differentiation and that reduction of bone mass in NEKO mice is due to impaired bone homeostasis by decreased osteoblast differentiation.

Discussion

It has been shown that the Keap1-deficient mouse is a useful model for the study of Nrf2 hyperactivation, the juvenile lethality of mice hampers uses of the mice (Wakabayashi et al, 2003). To overcome this difficulty, we recently generated alive model of Keap1-null mouse referred to as NEKO mouse (Suzuki et al, 2017). In this study, we examined pathophysiological contribution of Nrf2 activation to bone formation utilizing the NEKO mice. We found that hyperactivation of Nrf2 leads to low bone density. This novel phenotype of Nrf2 activation is independent of nephrogenic diabetes insipidus identified in NEKO mice in the previous study (Suzuki et al, 2017). Primary culture experiments using newborn calvarias cells from Keap1-null mice indicate that impaired osteoblast differentiation is responsible for bone hypoplasia caused by the Nrf2 hyperactivation. These results indicate that the Nrf2 hyperactivation leads to bone hypoplasia.

The finding that osteoblast differentiation of primary newborn calvarias cells is impaired by the Keap1-deficiency is consistent with the previous observation that Nrf2 overexpression in osteoblastic MC3T3 cells showed osteoblast differentiation defects (Hinoi et al, 2006). Nrf2 has been reported to interact with Runx2, a master transcription factor of osteoblastgenesis, and interferes with the Runx2-dependent transcriptional activation (Hinoi et al, 2006). Although Nrf2 in general acts as an activator (Katoh et al, 2001; Sekine et al, 2016), in certain context Nrf2 acts as a suppressor of gene expression; for instance, genes for inflammatory cytokines (Kobayashi et al, 2016). Therefore, the repressor function of Nrf2 for *Runx2* gene could be a plausible mechanism underlying the impaired osteoblastgenesis by Nrf2. Another report showed that some members of leucine zipper (bZIP) transcriptional factors. such as C/EBPβ and ATF4, are involved in osteoblastgenesis (He et al, 2001), implying that Nrf2 might compete with the other bZIP members for their binding sequence. Moreover, a recent report shows that Nrf2 activation impairs quiescence and bone marrow reconstitution capacity of hematopoietic stem cells (Murakami et al, 2017), implying that supply of osteoblasts may be impaired by the Nrf2 activation. Regarding for molecular mechanism of Nrf2-mediated suppression of osteoclastgenesis, we previously found that Keap1-deficient macrophages were unable to differentiate into osteoclasts *in vitro* via attenuation of RANKL-mediated signaling and expression of NFATc1 (nuclear factor of

activated T cells cytoplasmic 1) (Sakai et al, 2017).

In light of the use of Nrf2-inducing compounds as potential medical treatments, many studies have shown that pharmacological Nrf2 induction gives rise to a protective effect against a variety stresses, including ischemia-reperfusion injury (Nezu et al, 2017), carcinogenesis (Kensler and Wakabayashi, 2010) and inflammation (Keleku-Lukwete et al, 2017; Kobayashi et al, 2016). Although there are many papers that have assessed effects of Nrf2-induing chemicals (Kensler et al, 2013; Suzuki and Yamamoto, 2017), to our knowledge it has never been verified that such Nrf2 inducers provoke impairment of bone homeostasis. In this regard, we previous found that Nrf2 induction during development cause nephrogenic diabetes insipidus (Suzuki et al, 2017), but the Nrf2 induction during adulthood will not cause such adverse effects in the kidney. These observations suggest that the Nrf2-inducer treatment may have a critical period during development. Further investigation will be required to address whether Nrf2 is actually induced in bone cells under physiological or pathological conditions.

Of note, *de novo* mutations in human NRF2 gene that induce NRF2 were recently identified (Huppke et al, 2017), and the cases with the NRF2 induction displayed mild developmental delay, short stature and delayed bone age (Huppke et al, 2017). The phenotypes observed in the cases are consistent with the phenotype we have observed in the NEKO mice, including the small body length and low bone density. These observations in human cases and in NEKO mouse analysis in combination support the contention that the Nrf2 hyperactivation in certain developmental window leads to the impairment of bone formation and homeostasis.

Experimental procedures

Mice

Generation of esophageal Nrf2-deficient and systemic Keap1-null mice (NEKO, *Keap1*$^{-/-}$*::Nrf2*$^{Flox/Flox}$*::Keratin5-Cre*) and renal tubule-specific Keap1 knockout mice (Keap1 TKO, *Keap1*$^{Flox/Flox}$*::Pax8-rtTA::TetO-Cre*) were described previously (Suzuki et al, 2017). For analysis of NEKO mice, littermate mice (*Nrf2*$^{Flox/Flox}$*::K5-Cre:Keap1*$^{+/-}$ or *Nrf2*$^{Flox/Flox}$*::Keap1*$^{+/-}$) were used as controls. For analysis of Keap1 TKO mice, littermate mice (*Keap1*$^{Flox/Flox}$ *or Keap1*$^{Flox/Flox}$*::Pax8-rtTA*) were used as controls. Pregnant female mice were fed with 1-mg/ml doxycyline (DOX) in the drinking water. Blood samples were collected from the mice and analyzed using iSTAT-1 analyzer (Abott) for blood ionized calcium (Ca) level. All mice were kept in specific-pathogen-free conditions and were treated according to the regulations of *The Standards for Human Care and Use of Laboratory Animals of Tohoku University* and *Guidelines for Proper Conduct of Animal Experiments* of the Ministry of Education, Culture, Sports, Science, and Technology of Japan.

Osteoblast differentiation culture

For *in vitro* osteoblast differentiation, newborn calvarias were digested with 1-mg/ml collagenase (Wako) and 2-mg/mL Dispase (Gibco) at 37°C for 15 minutes with the repeat of this at least 5 times. The cells were then cultured with α-MEM (Wako) with 10% FBS for 5-7 days. After primary culture cells were treated with 0.25% Trypsin-EDTA solution (Sigma), cells were cultured in osteogenic medium (50-μM ascorbic acid, 10-nM dexamethasone, and 10-mM β-glycerophosphate) for 14 days. For quantifying alkaline phosphatase (ALP) activity, ALP assay was performed as described (Nishikawa et al, 2010). For quantitative analysis, the densities of scanned images of stained plate were measured using Image J software.

Osteoclast differentiation culture

The *in vitro* osteoclast differentiation was conducted as described (Nishikawa et al, 2010). Briefly, bone marrow cells were flushed out from femur and tibia of female mice in each genotype at 7-10 weeks. The cells were cultured in 10% FBS-αMEM with 10

ng/ml of M-CSF (R&D Systems) for 2 days, and osteoclast precursor cells were obtained. The cells were cultured in 10% FBS-αMEM with 50-ng/ml RANKL (Oriental Yeast) in the presence of 10-ng/ml M-CSF for additional 5 days. Quantification of tartrate-resistant acid phosphatase (TRAP) activity was performed by TRACP & ALP double-stain Kit (Takara). To evaluate osteoclast differentiation, TRAP-positive multi-nucleated cells were counted as mature osteoclasts. For quantitative analysis, the densities of scanned images of stained plate were measured using Image J software.

Microcomputed tomography analysis

Whole body or full length of femur of several stage female mice was μCT scanned with a Latheta LCT-200 (Hitachi-Aloka) to analyze bone shape, lipid volume and bone morphometry. Three-dimensional reconstruction images of bone were obtained by Amira (M@xnet).

Alcian blue staining

Fumures were fixed in 70% ethanol, decalcified paraffin-embedded, and sectioned to stain with alcian blue. For quantitative analysis, the densities and thickness of scanned images were measured using Image J software.

Statistical analyses

Data are expressed as the mean ± SD. For statistical analysis, pairwise comparisons were made by Mann-Whitney *U* test. *P*-values < 0.05 were considered statistically significant.

Acknowledgments

We thank the Biomedical Research Core of Tohoku University Graduate School of Medicine for technical support. This work was supported in part by grants from JSPS KAKENHI 26460354, 26111010 and 17K15590 to T.S., 26111002 to M.Y., AMED-CREST (chronic inflammation) to M.Y..

References

Asagiri, M. & Takayanagi, H. (2007) The molecular understanding of osteoclast differentiation. *Bone* **40**, 251-264.

Bai, X.C., Lu, D., Bai, J., Zheng, H., Ke, Z.Y., Li, X.M. & Luo, S.Q. (2004) Oxidative stress inhibits osteoblastic differentiation of bone cells by ERK and NF-kappaB. *Biochem Biophys Res Commun* **314**, 197-207.

Gogakos, A.I., Duncan Bassett, J.H. & Williams, G.R. (2010) Thyroid and bone. *Arch Biochem Biophys* **503**, 129-136.

He, C.H., Gong, P., Hu, B., Stewart, D., Choi, M.E., Choi, A.M. & Alam, J. (2001) Identification of activating transcription factor 4 (ATF4) as an Nrf2-interacting protein. Implication for heme oxygenase-1 gene regulation. *J Biol Chem* **276**, 20858-20865.

Hinoi, E., Fujimori, S., Wang, L., Hojo, H., Uno, K. & Yoneda, Y. (2006) Nrf2 negatively regulates osteoblast differentiation via interfering with Runx2-dependent transcriptional activation. *J Biol Chem* **281**, 18015-18024.

Huppke, P., Weissbach, S., Church, J.A. *et al.* (2017) Activating de novo mutations in NFE2L2 encoding NRF2 cause a multisystem disorder. *Nat Commun* **8**, 818.

Hyeon, S., Lee, H., Yang, Y. & Jeong, W. (2013) Nrf2 deficiency induces oxidative stress and promotes RANKL-induced osteoclast differentiation. *Free Radic Biol Med* **65**, 789-799.

Itoh, K., Chiba, T., Takahashi, S., Ishii, T., Igarashi, K., Katoh, Y., Oyake, T., Hayashi, N., Satoh, K., Hatayama, I., Yamamoto, M. & Nabeshima, Y. (1997) An Nrf2/small Maf heterodimer mediates the induction of phase II detoxifying enzyme genes through antioxidant response elements. *Biochem Biophys Res Commun* **236**, 313-322.

Jun, J.H., Lee, S.H., Kwak, H.B., Lee, Z.H., Seo, S.B., Woo, K.M., Ryoo, H.M., Kim, G.S. & Baek, J.H. (2008) N-acetylcysteine stimulates osteoblastic differentiation of mouse calvarial cells. *J Cell Biochem* **103**, 1246-1255.

Katoh, Y., Itoh, K., Yoshida, E., Miyagishi, M., Fukamizu, A. & Yamamoto, M. (2001) Two domains of Nrf2 cooperatively bind CBP, a CREB binding protein, and synergistically activate transcription. *Genes Cells* **6**, 857-868.

Keleku-Lukwete, N., Suzuki, M. & Yamamoto, M. (2017) An Overview of the Advantages of KEAP1-NRF2 System Activation During Inflammatory Disease Treatment. *Antioxid Redox Signal*.

Kensler, T.W., Egner, P.A., Agyeman, A.S., Visvanathan, K., Groopman, J.D., Chen, J.G., Chen, T.Y., Fahey, J.W. & Talalay, P. (2013) Keap1-nrf2 signaling: a target for cancer prevention by sulforaphane. *Top Curr Chem* **329**, 163-177.

Kensler, T.W. & Wakabayashi, N. (2010) Nrf2: friend or foe for chemoprevention? *Carcinogenesis* **31**, 90-99.

Kobayashi, A., Kang, M.I., Okawa, H., Ohtsuji, M., Zenke, Y., Chiba, T., Igarashi, K. & Yamamoto, M. (2004) Oxidative stress sensor Keap1 functions as an adaptor for Cul3-based E3 ligase to regulate proteasomal degradation of Nrf2. *Mol Cell Biol* **24**, 7130-7139.

Kobayashi, E.H., Suzuki, T., Funayama, R., Nagashima, T., Hayashi, M., Sekine, H., Tanaka, N., Moriguchi, T., Motohashi, H., Nakayama, K. & Yamamoto, M. (2016) Nrf2 suppresses macrophage inflammatory response by blocking proinflammatory cytokine transcription. *Nat Commun* **7**, 11624.

Lean, J.M., Davies, J.T., Fuller, K., Jagger, C.J., Kirstein, B., Partington, G.A., Urry, Z.L. & Chambers, T.J. (2003) A crucial role for thiol antioxidants in estrogen-deficiency bone loss. *J Clin Invest* **112**, 915-923.

Manolagas, S.C. (2000) Corticosteroids and fractures: a close encounter of the third cell kind. *J Bone Miner Res* **15**, 1001-1005.

Mody, N., Parhami, F., Sarafian, T.A. & Demer, L.L. (2001) Oxidative stress modulates osteoblastic differentiation of vascular and bone cells. *Free Radic Biol Med* **31**, 509-519.

Murakami, S., Suzuki, T., Harigae, H., Romeo, P.H., Yamamoto, M. & Motohashi, H. (2017) NRF2 Activation Impairs Quiescence and Bone Marrow Reconstitution Capacity of Hematopoietic Stem Cells. *Mol Cell Biol* **37**.

Nezu, M., Souma, T., Yu, L., Suzuki, T., Saigusa, D., Ito, S., Suzuki, N. & Yamamoto, M. (2017) Transcription factor Nrf2 hyperactivation in early-phase renal ischemia-reperfusion injury prevents tubular damage progression. *Kidney Int* **91**, 387-401.

Nishikawa, K., Nakashima, T., Takeda, S., Isogai, M., Hamada, M., Kimura, A., Kodama, T., Yamaguchi, A., Owen, M.J., Takahashi, S. & Takayanagi, H. (2010) Maf promotes osteoblast differentiation in mice by mediating the age-related switch in mesenchymal cell differentiation. *J Clin Invest* **120**, 3455-3465.

Sakai, E., Morita, M., Ohuchi, M., Kido, M.A., Fukuma, Y., Nishishita, K., Okamoto, K., Itoh, K., Yamamoto, M. & Tsukuba, T. (2017) Effects of deficiency of Kelch-like ECH-associated protein 1 on skeletal organization: a mechanism for diminished nuclear factor of activated T cells cytoplasmic 1 during osteoclastogenesis. *FASEB J* **31**, 4011-4022.

Sekine, T., Hirata, T., Mine, T. & Fukano, Y. (2016) Activation of transcription factors in human bronchial epithelial cells exposed to aqueous extracts of mainstream cigarette smoke in vitro. *Toxicol Mech Methods* **26**, 22-31.

Suzuki, T., Motohashi, H. & Yamamoto, M. (2013) Toward clinical application of the Keap1-Nrf2 pathway. *Trends Pharmacol Sci* **34**, 340-346.

Suzuki, T. & Yamamoto, M. (2015) Molecular basis of the Keap1-Nrf2 system. *Free Radic Biol Med* **88**, 93-100.

Suzuki, T., Seki, S., Hiramoto, K., Naganuma, E., Kobayashi, E.H., Yamaoka, A., Baird, L., Takahashi, N., Sato, H. & Yamamoto, M. (2017) Hyperactivation of Nrf2 in early tubular development induces nephrogenic diabetes insipidus. *Nat Commun* **8**, 14577.

Suzuki, T. & Yamamoto, M. (2017) Stress-sensing mechanisms and the physiological roles of the Keap1-Nrf2 system during cellular stress. *J Biol Chem* **292**, 16817-16824.

Wakabayashi, N., Itoh, K., Wakabayashi, J., Motohashi, H., Noda, S., Takahashi, S., Imakado, S., Kotsuji, T., Otsuka, F., Roop, D.R., Harada, T., Engel, J.D. & Yamamoto, M. (2003) Keap1-null mutation leads to postnatal lethality due to constitutive Nrf2 activation. *Nat Genet* **35**, 238-245.

Figure legends

Figure 1 NEKO mice show small body and femur length

(A, B) X-ray photographs of whole mouse body of control (A) and NEKO (B) littermate male mice at 8-10 weeks. Scale bars, 1.5 cm. (C) The representative femur appearance of control (left) and NEKO (right) mice. Right femur of male mice at 8-10 weeks. Scale bars, 5 mm. (D) Femur length from proximal end of macro-nodular or femur head to the distal end of femur of control (n=6) and NEKO (n=6) male mice. *p<0.05.

Figure 2 NEKO mice show decreased bone mass compared to control mice

(A-D) Three-dimensional re-constructional images of femurs from μCT analysis obtained from 8-10 week-old control and NEKO male mice. (A, B) Representative overview of femur. Scale bars, 2.5 mm. (C, D) The representative cross sections of distal femur at 0.3-0.8 mm above the distal growth plate. Scale bars, 500 μm. (E-G) Bone morphometric parameters assessed with a μCT analysis program of femur of 8-10 week-old control (n=3) and NEKO (n=3) male mice. (E) Average cortical thickness (Ct. Th) of control (black) and NEKO (red) mice. (F) Volume bone mineral density (vBMD) of control (black) and NEKO (red) mice. (G) Cortical bone tissue mineral density (CB. TMD) of control (black) and NEKO (red) mice. Data are means ± SE. *p<0.05, **p<0.01. (H) Blood ionized calcium (Ca) level in control (n=5) and NEKO (n=6) mixed-gender mice at 3-6 weeks of age. Data are means ± SE. **p<0.01.

Figure 3 Nrf2 activation suppresses both osteoclastgenesis and osteoblastgenesis

(A) Osteoclast differentiation protocol. Osteoclast progenitor cells were obtained from femur of 6-8-week-old NEKO and control littermate mixed gender mice, and were cultured with M-CSF and RANKL. (B, C) Representative images of cultured osteoclasts obtained from femur of control (B) and NEKO (C) mixed gender mice were subjected to TRAP staining. Scale bars, 100 μm. (D) Relative intensity of TRAP staining of cultured osteoclasts obtained from femur of control (n=3) and NEKO (n=3) mice. Data are means ± SE. *p<0.05. (E) Osteoblast differentiation protocol.

Newborn calvarias were digested with collagenase and Dispase, and harvested in α-MEM medium. After several passages, the osteoblast cells were cultured with osteoblast differentiation medium. *Keap1*$^{+/-}$ and *Keap1*$^{-/-}$ osteoblast cells were cultured with ascorbic acid, ß-glycerophosphate and dexamethasone for 14 days. (E) Cultured cells were stained with ALP staining at each time point. Representative data are shown. (F) Relative intensity of ALP staining of cultured osteoblasts obtained from *Keap1*$^{+/-}$ (n=3) and *Keap1*$^{-/-}$ (n=3) mice. Data are means ± SE. *p<0.05.

Figure S1

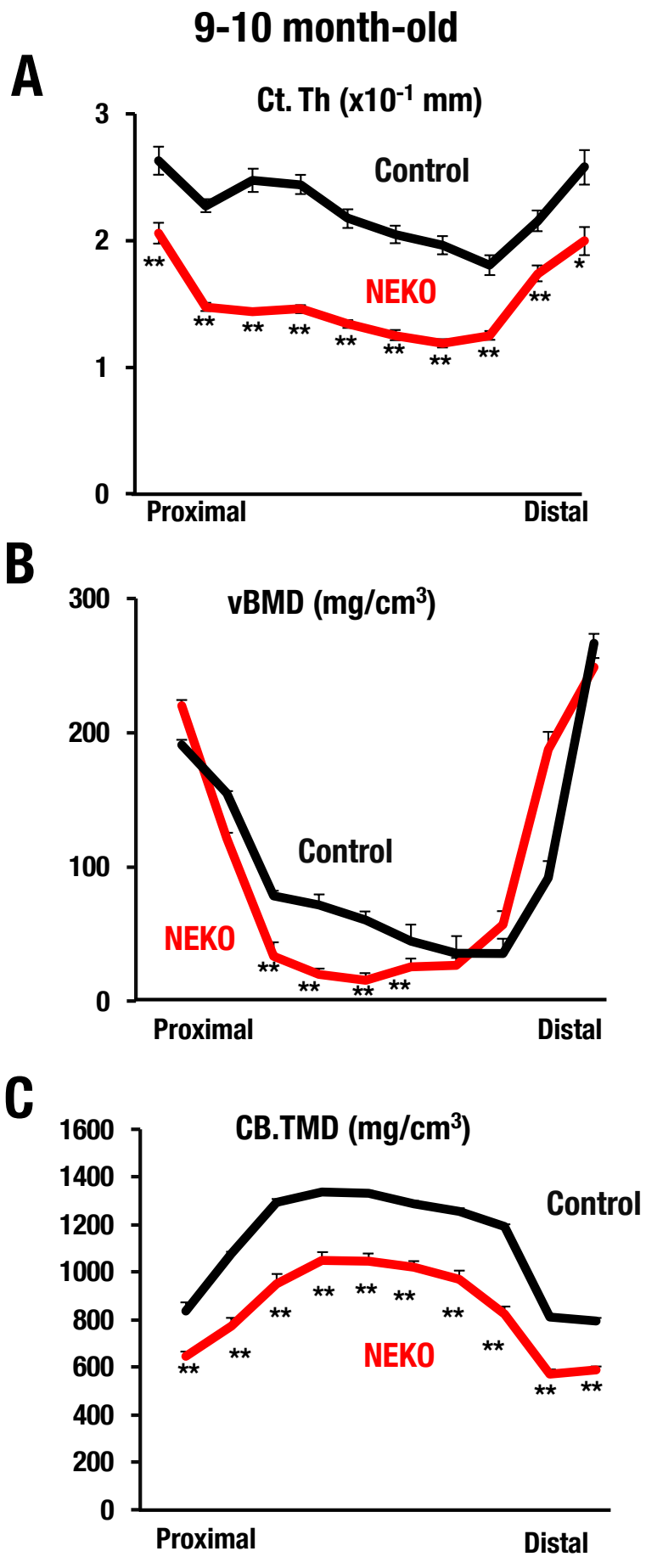
9-10 month-old
A
Ct. Th (x10-1 mm)
Control
NEKO
Proximal
Distal
B
vBMD (mg/cm3)
Control
NEKO
Proximal
Distal
C
CB.TMD (mg/cm3)
Control
NEKO
Proximal
Distal

Figure S2

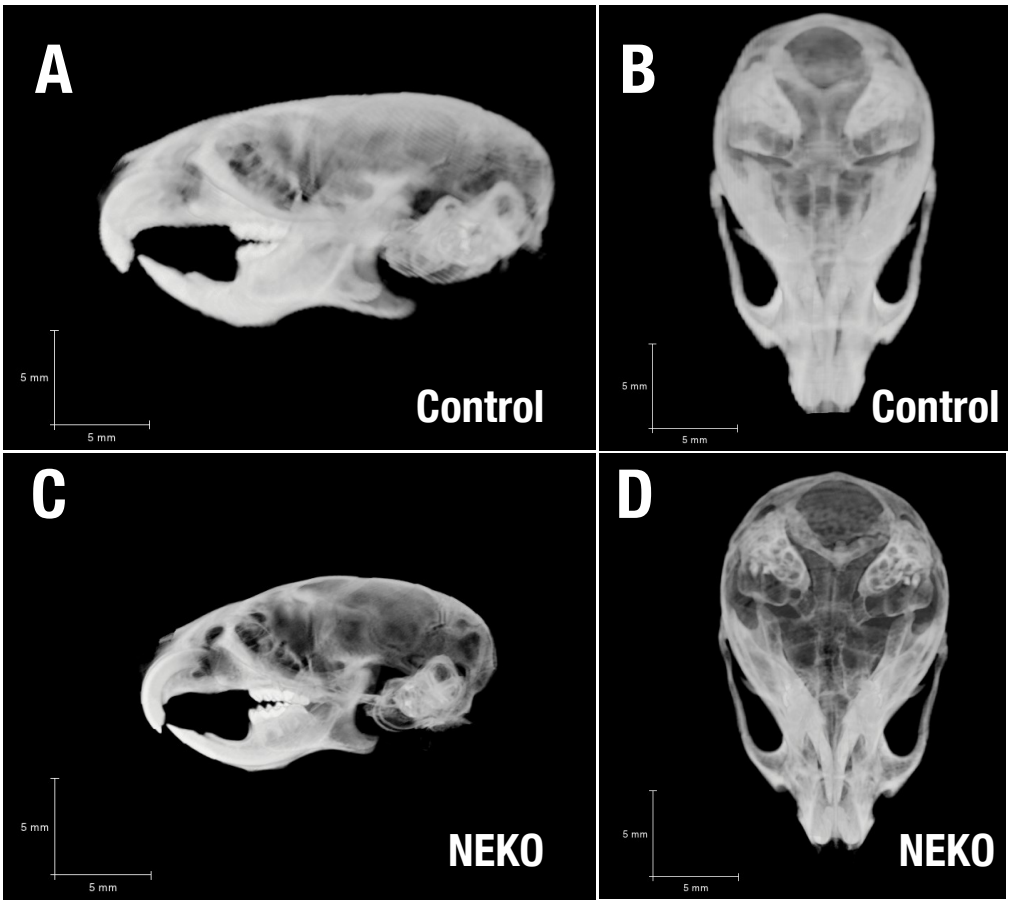
A
5 mm
5 mm
Control
B
5 mm
5 mm
Control
C
5 mm
5 mm
NEKO
D
5 mm
5 mm
NEKO

Figure S3

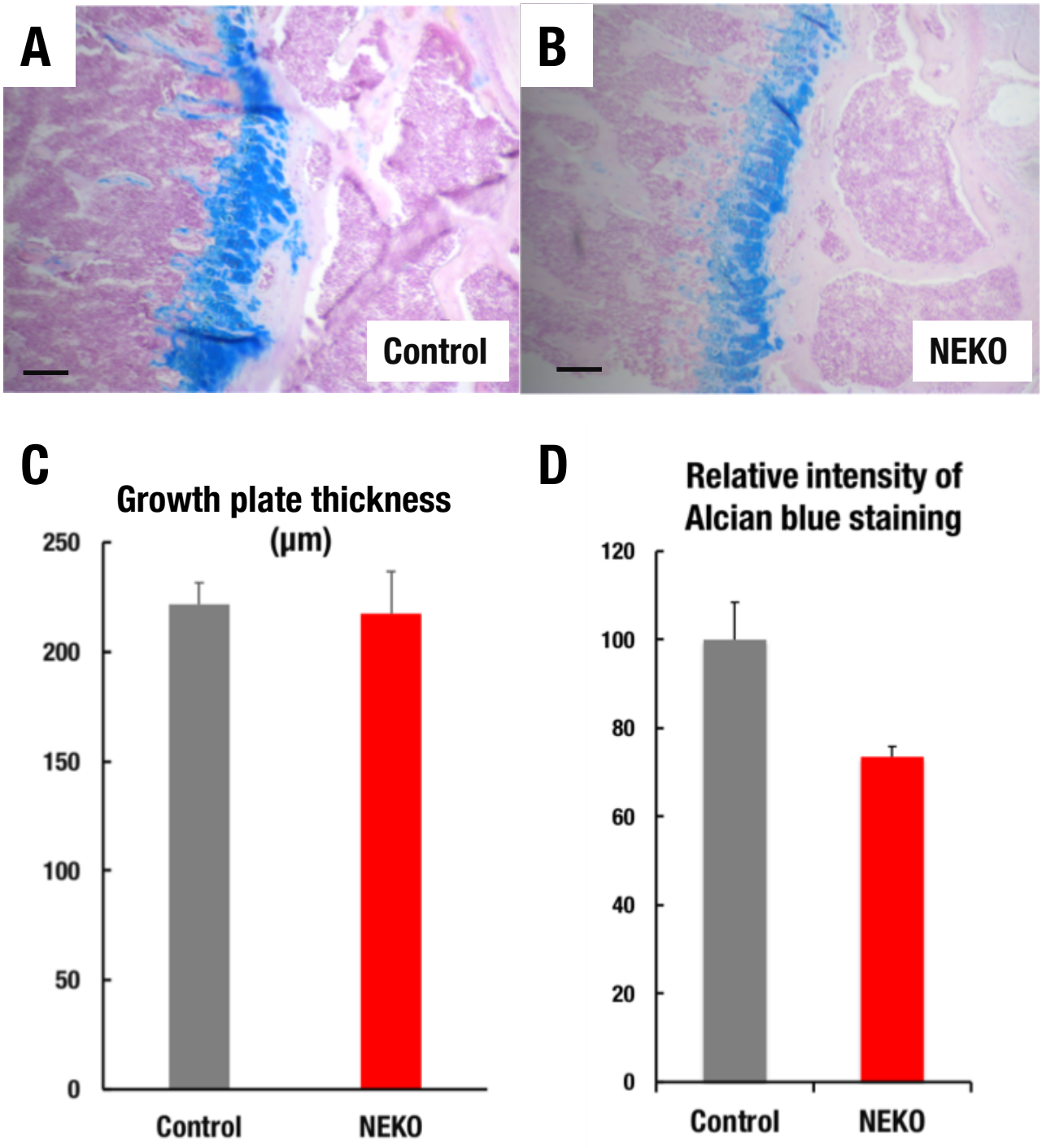
A
Control
B
NEKO
C
Growth plate thickness
(μm)
250
200
150
100
50
0
Control
NEKO
D
Relative intensity of
Alcian blue staining
120
100
80
60
40
20
0
Control
NEKO

Figure S4


A
Control
Keap1 TKO

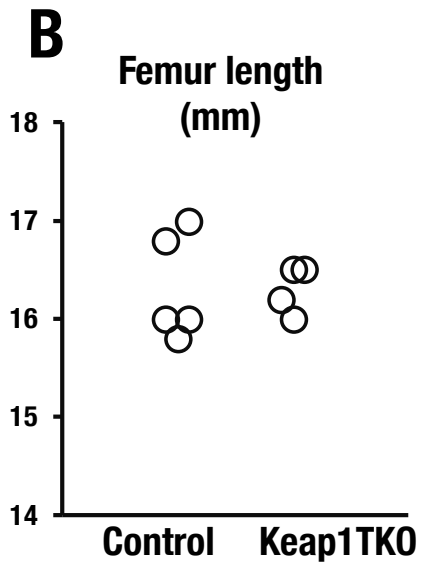
B
Femur length
(mm)
18
17
16
15
14
Control
Keap1TKO

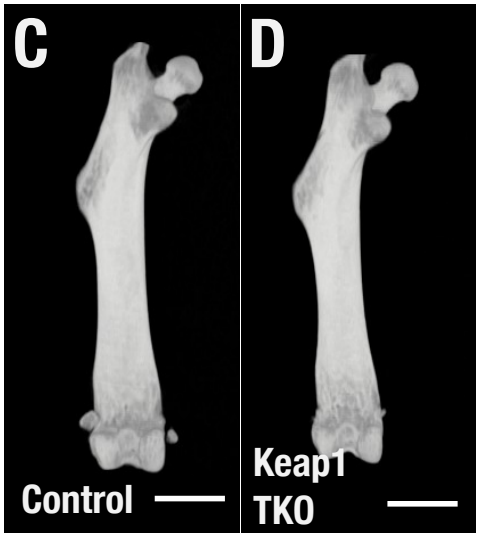
C
D
Control
Keap1
TKO

Figure S5

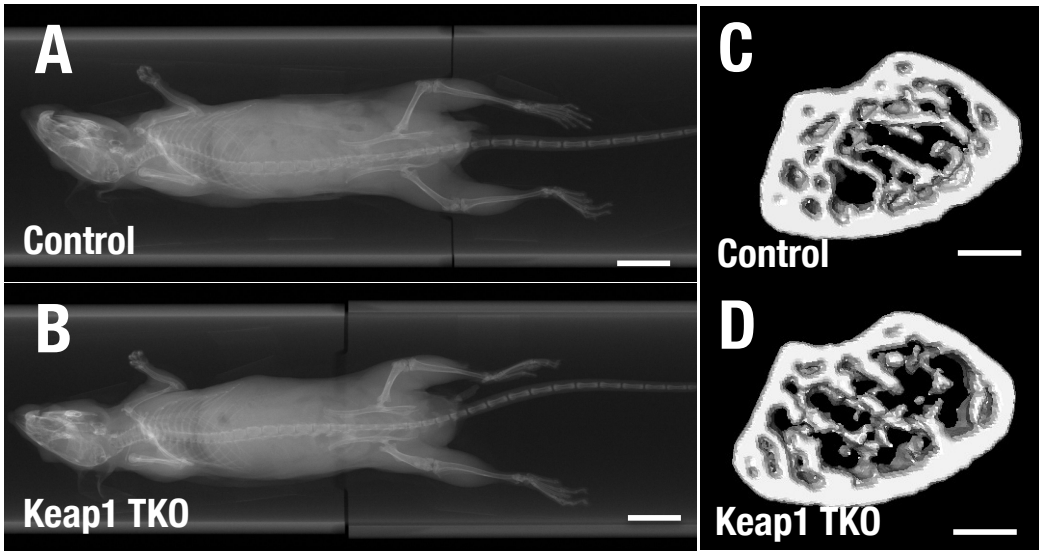
A
Control
B
Keap1 TKO
C
Control
D
Keap1 TKO

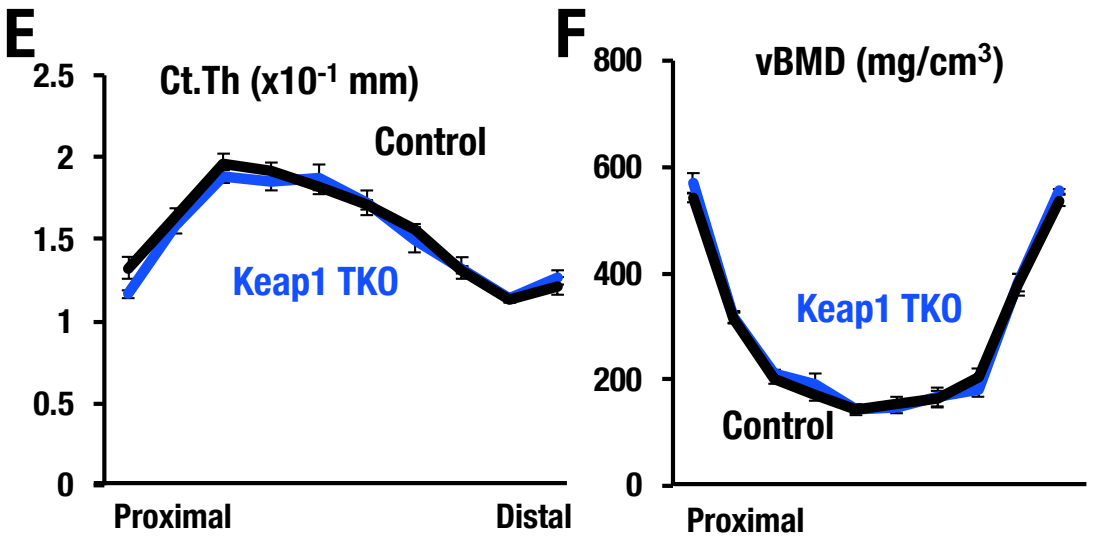
E
Ct.Th (x10-1 mm)
2.5
2
1.5
1
0.5
0
Control
Keap1 TKO
Proximal
Distal
F
vBMD (mg/cm3)
800
600
400
200
0
Keap1 TKO
Control
Proximal

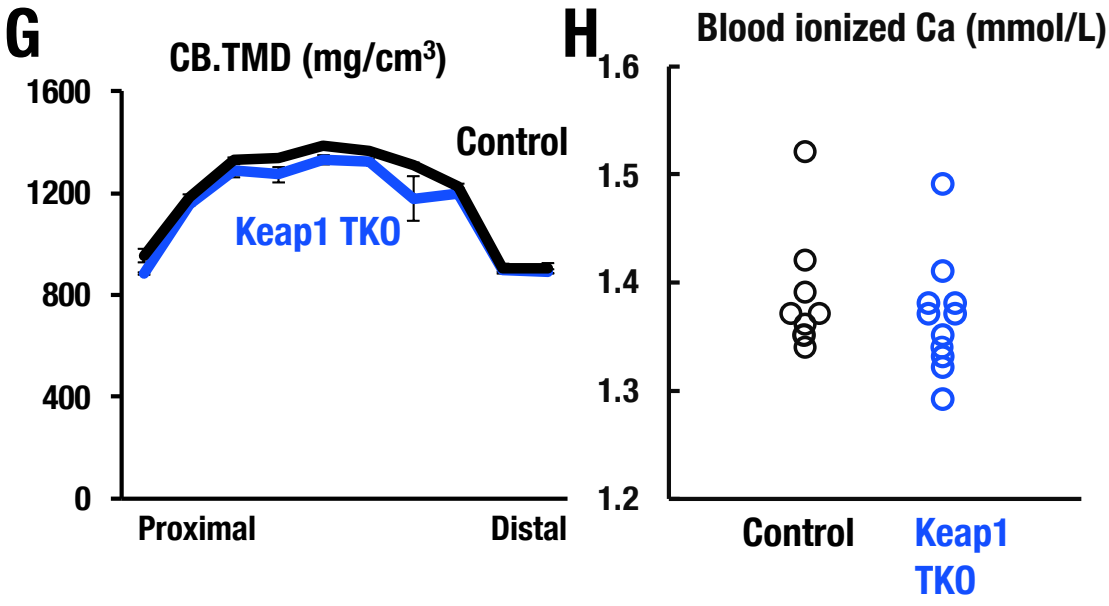
G
CB.TMD (mg/cm3)
1600
1200
800
400
0
Control
Keap1 TKO
Proximal
Distal
H
Blood ionized Ca (mmol/L)
1.6
1.5
1.4
1.3
1.2
Control
Keap1 TKO

Figure S1

(A-C) μCT bone morphometric parameters of femur of control (n=3) and NEKO (n=3) male mice at 9-10 months. (A) Average cortical thickness (Ct. Th) of control (black) and NEKO (red) mice. (B) Volume bone mineral density (vBMD) of control (black) and NEKO (red) mice. (C) Cortical bone tissue mineral density (CB. TMD) of control (black) and NEKO (red) mice. Data are means ± SE. *p<0.05, **p<0.01.

Figure S2

(A-D) Three-dimensional reconstruction images of side view (A, C) and front view (B, D) of skulls from control (A, B) and NEKO (C, D) female mice at 8-10 weeks.

Figure S3

(A, B) Representative images of Alcian blue staining of femur growth plate obtained from control (A) and NEKO (B) male mice at 8-10 weeks. Scale bars, 100 μm. (C) Femur growth plate thickness of control and NEKO male mice at 8-10 weeks. (D)

Figure S4

Macroscopic view (A), length (B) and three-dimensional re-constructional images (C, D) of femurs from control (n=5) and Keap1 TKO (n=4) male mice at 21-28 weeks. Scale bars indicate 5.0 mm (A) and 2.5 mm (C, D).

Figure S5

(A, B) Whole body X-ray photographs of control and Keap1 TKO littermate male mice at 21-28 weeks. Scale bars, 1.5 cm. (C, D) Three-dimensional reconstruction images of cross-section of distal femur at 0.3-0.8 mm above the growth plate. Scale bars, 500 μm. (E-G) Bone morphometric parameters of control (n=4) and Keap1 TKO (n=5) mice at 21-28 weeks. (E) Average cortical thickness (Ct. Th) of control (black) and Keap1 TKO (blue) mice, (F) Volume bone mineral density (vBMD) of control (black) and Keap1 TKO (blue) mice. (G) Cortical bone tissue mineral density (CB. TMD) of control (black) and Keap1 TKO (blue) mice. Data are means ± SE. (H) Blood ionized calcium (Ca) level in control (n=8) and Keap1 TKO (n=11) mixed-gender mice. Data are means ± SE.